Green Chemistry

Accepted Manuscript

ROYAL SOCIETY OF CHEMISTRY

www.rsc.org/greenchem

Green Chem. RSCPublishing

ARTICLE

Ruthenium-containing β-cyclodextrin polymer globules for the catalytic hydrogenation of biomass-derived furanic compounds

Cite this: DOI: 10.1039/x0xx00000x

Received 00th January 2014,
Accepted 00th January 2014

DOI: 10.1039/x0xx00000x

www.rsc.org/

R. Herbois,[a,b] S. Noël,[a,b] B. Léger,[a,b] S. Tilloy,[a,b] S. Menuel,[a,b] A. Addad,[c] B. Martel,[c] A. Ponchel[a,b] and E. Monflier*[a,b]

The confinement of catalytically active metallic nanoparticles within discrete and robust microenvironments was successfully achieved by using a water-compatible three-dimensional β-cyclodextrin-based polymer. The strategy was examined using ruthenium through an aqueous colloidal approach involving the chemical reduction of ruthenium nitrosyl nitrate by sodium borohydride in the presence of a water-soluble β-CD polymer crosslinked with citric acid (poly(CTR-β-CD). The advantage of this polymer for nanoparticles synthesis is *i)* to exert additional stabilizing effects through steric interactions (crosslinked chains and β-cyclodextrin entities) and electrostatic interactions (ionisable–COOH groups) and *ii)* to provide accessible nanopockets between the stable junctions of the polymer skeleton. The poly(CTR-β-CD) Ru(0) system was characterized at different stages of the synthesis by combining proton nuclear magnetic resonance spectroscopy, dynamic light scattering and transmission electron microscopy measurements. The results highlighted that, in contrast with a series of control colloidal ruthenium catalysts, the specific use of poly(CTR-β-CD) allowed not only the stabilization of smaller size-controlled ruthenium nanoparticles (approximately 1.8 nm) but also their confinement in individual superstructures having sizes mostly in the range of 50 to 100 nm. These polymer-encapsulated ruthenium nanoparticles were applied as catalysts for the aqueous phase hydrogenation of biomass-derived 2-furaldehyde and 3-(2-furyl)acrolein under mild reaction conditions, i.e. 303 K and 1 MPa. The high reactivity was related to the presence of individual globular objects acting as catalytic "microreactors", in which the consecutive hydrogenation reactions and product/substrate diffusional exchanges can occur efficiently in the confined spaces. The robustness of the system was demonstrated through recycling experiments and TEM characterizations after catalytic tests.

Introduction

Over the past decade, transition metal nanoparticles (NPs) with narrow size distributions have attracted a great deal of attention in a wide range of applications, such as catalysis.[1-4] In a general viewpoint, metal NPs are known to exhibit unique properties that cannot be achieved by their bulk counterparts. These systems are known to provide a high surface area of catalytically active metal thanks to a large fraction of surface-exposed metal atoms and high number edges and defects, at which catalysis usually takes place. However, it is generally assumed that the most important drawback of transition metal NPs is their tendency to aggregate, leading to loss of the major part of their characteristics. An effective way to solve this problem is to stabilize the NPs by immobilizing them on a solid support (e.g. inorganic oxides, porous carbons or insoluble polymers)[5-8] or by using soluble capping agents (e.g. surfactants, ligands or polymers).[9-11]

In recent years, a number of studies has utilized the ability of specially nanostructured polymers to serve as matrices with confined cavities, in which nanoparticles can be accommodated and protected against aggregation while facilitating the exchanges between the interior and exterior of the polymeric environment. Thus, utilization of micelles-forming block co-polymers,[12-14] and dendrimers[15,16] have been employed as structures capable of incorporating metallic nanoparticles active in catalysis. Pertinent examples can be found in several excellent reviews.[17,18] For instance, El-Sayed and coworkers reported for the first time the use of different generations (G2-G4) of poly(amidoamine) dendrimers bearing hydroxyl groups (PAMAMOH) to encapsulate Pd NPs for their use in Suzuki cross-coupling.[15]

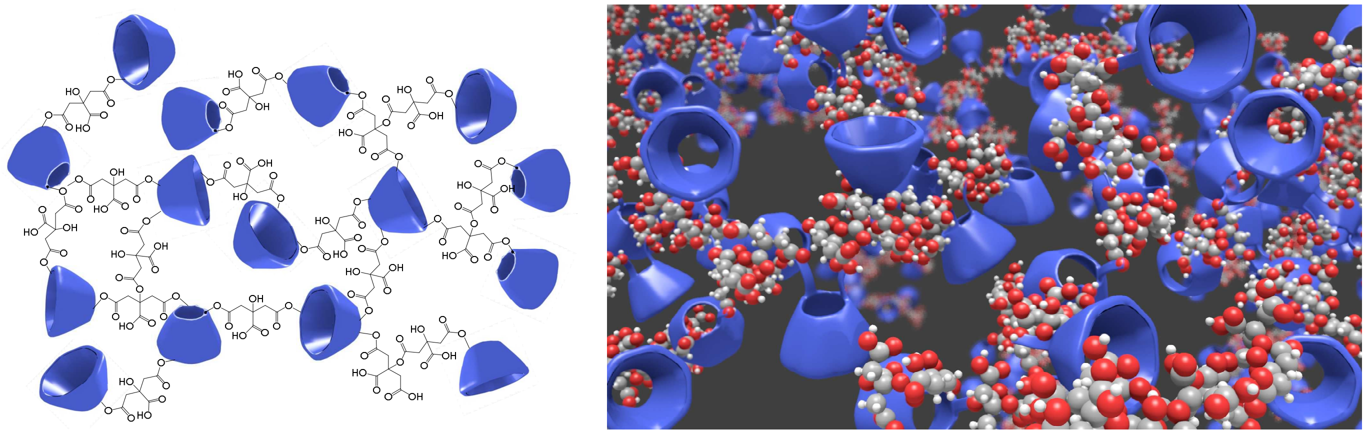

Scheme 1 Schematic structures of the poly(CTR-β-CD) polymer in a two-dimensional representation (left) and in a three-dimensional imaging using 3D Modeling Blender Software (right)

In the case of low-generation dendrimers (G2 and G3), the less dense structure was favorable to the catalytic activity whereas conversely G4 dendrimer resulted in a lower activity due to a lower substrate accessibility. Interestingly also, it has been reported by the group of Schubert that well-defined palladium NPs with a diameter of about 4 nm could be stabilized inside a five-arm star-shaped block copolymer formed of a poly(ethylene oxide) (PEO) core and a poly(ε-caprolactone) (PCL) corona.[19] Reduction of the palladium acetate was performed with $NaBH_4$ and the reaction was supposed to occur preferentially in the hydrophilic PEO core of the star-shaped copolymer. These NPs were found to efficiently catalyze the Heck coupling of styrene with 4-bromoacetophenone.

upplied by Aldrich Chemicals and used as received. Purified developing efficient chemical transformations under environmentally benign conditions. For this purpose, water-soluble polymer scaffolds modified with complementary recognition units, such as cyclodextrins, constitute an attractive system to control the growth and dispersion of metal nanoparticles in aqueous colloidal suspensions.[20-23] We report herein that three-dimensional cross-linked cyclodextrins polymers can be used as matrices to stabilize and confine metal nanoparticles into a microenvironment. β-cyclodextrin (β-CD) is a torus-shaped cyclic oligosaccharide composed of seven α-D-glucopyranose units forming a rigid cavity and a high number of reactive hydroxyl groups available for cross-linking. The fabrication of cyclodextrin polymers exhibiting an interconnected nanoporosity has already been described in the literature *via* the use of epoxides, epichlorohydrin, activated carbonyl compounds pyromellitic dialdehydes, polycarboxylic acids as cross-linking agents.[24,25] The choice of the cross-linking agent and degree of cross-linking is known to influence the behavior of the polymer in terms of water-solubility and swellability. Thus for instance, high cross-linked polymers formed by the polycondensation of cyclodextrins in a three-dimensional network have recently emerged as versatile nanosponge systems with high efficiency for drug delivery, pollutants removal and chiral photoreaction.[26-28] Surprisingly and to the best of our knowledge the use of cross-linked polymers as a stabilization medium for the synthesis of catalytically active metal nanoparticles has been scarcely investigated.[29]

The strategy has been examined with the synthesis of monodisperse borohydrate-reduced ruthenium NPs, starting from ruthenium nitrosyl nitrate ($Ru(NO)(NO_3)_3$) as the metal precursor and a cyclodextrin polymer, which is denoted as poly(CTR-β-CD), as the protective polymer. Poly(CTR-β-CD) is a three-dimensional polymer (3D-polymer) resulting from the controlled polyesterification between native β-cyclodextrin and citric acid (CTR). From environmental viewpoint, its synthesis has the great advantage of using only non-toxic and water-soluble reagents, therefore avoiding the need of additional organic solvents. The ability of poly(CTR-β-CD) 3D-polymer to specifically promote the stabilization of small size-controlled Ru(0) NPs within discrete spherical microdomains will be discussed on the basis of proton nuclear magnetic resonance spectroscopy (^{1}H NMR), dynamic light scattering (DLS), and transmission electron microscopy (TEM) measurements and compared to behavior of other water-soluble control stabilizing systems. The catalytic activity of the poly(CTR-β-CD) Ru(0) NPs will be finally evaluated in the aqueous hydrogenation of 2-furaldehyde and 3-(2-furyl)acrolein selected as model compounds of biomass-derived-feedstocks. Indeed, furan-based derivatives are important chemicals readily accessible from pentosan-rich biomass and appear as key chemical intermediates for the synthesis of bio-based products through catalytic processes,[30-33] with applications in the field of fine chemicals, polymers and biofuels.[34-36]

Results and Discussion

Synthesis and characterization

The synthesis of poly(CTR-β-CD) 3D-polymer was carried out in the dried state at 140°C according to a method previously reported.[37] Briefly, the process consists of the polyesterification of CTR with β-CD in the presence of NaH_2PO_2 as catalyst at a respective weight ratio of CTR/β-CD/catalyst of 10/10/3. Then, the water-soluble fraction of the polymer is quantitatively recovered upon addition of water, dialyzed against water (6,000-8,000 Da cellulosic membranes) and finally lyophilized in order to obtain a white powder. The average molecular weight of poly(CTR-β-CD) based on gel permeation chromatogram analysis is MW = 25000 with a polydispersity index of 2.2 while the rate of incorporation of β-CD in the polymer determined by peak integration in the ^1H NMR spectrum is estimated to be 49 wt. % (Fig. 1, spectrum a.). The calculation method is given in the Supplementary material. Note that the peaks at $\delta = 6.11$ and 7.85 ppm are attributed to a small quantity of *cis* and *trans*-isomers of aconitic acid units formed as side-products during the dehydration of citric acid at 140°C (7 wt. %).[38] Additionally, an acid-base titration of poly(CTR-β-CD) gives 4.05 mmol g^{-1} acidic sites with a mean pKa value of 4.1 (Fig. S1 in the Supporting Information), which is coherent with the presence of available carboxylic acid groups within the cross-linked polymer. Taken together, the physicochemical characteristics of poly(CTR-β-CD) are of interest for providing a suitable environment to stabilize metal NPs through steric interactions (polymer and β-CD) and electrostatic interactions (ionisable–COOH groups) but also to confine them within pockets formed by the stable junctions of 3D-polymer network, as schematically represented in Scheme 1.

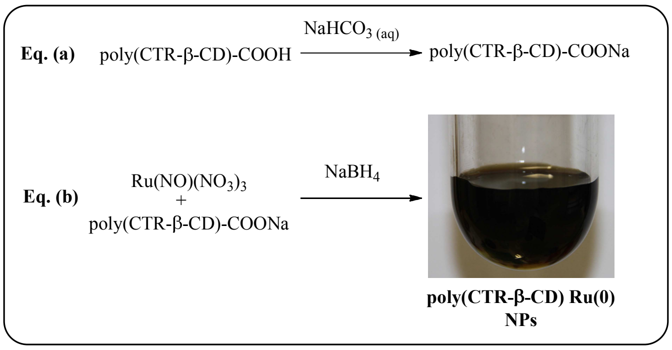

Scheme 2 Synthesis of Ru(0) NPs stabilized by poly(CTR-β-CD)

Concerning the synthesis of poly(CTR-β-CD)-protected ruthenium NPs, the current procedure is a slightly modified version of a published method[39,40] and is carried out in two successive steps (Scheme 2). In the first step [Equation (a)], 100 mg of poly(CTR-β-CD) is solubilized in an aqueous solution of $NaHCO_3$ (molar ratio of $NaHCO_3$ to COOH = 1) to convert the carboxylic acid groups into the corresponding sodium carboxylate salts, with respect to a pH value of approximately 6.1. The mixture is kept under constant stirring at room temperature for 3 hours. In the second step [(Equation b)], the ruthenium salt (40 μmol) is added to the deprotonated polymer and the mixed solution is stirred for an additional 30 minutes before the introduction of sodium borohydride as reducing agent (10 equiv. per mole of Ru)†. The color of the reaction medium changes upon addition of $NaBH_4$ from orange to dark brown due to the reduction of Ru(III) to Ru(0) while the pH varies between 6.1 and 8.1. The resulting colloidal dispersion is visually stable for months and no sedimentation is observed.

In addition, ^1H NMR experiments carried out in D_2O in the presence of poly(CTR-β-CD) at different points of the preparation (i.e. *after the consecutive addition of the following reactants,* $NaHCO_3$*,* $Ru(NO)(NO_3)_3$ *and* $NaBH_4$) have not revealed major changes in the 3.3-5.5 ppm region, which is ascribed to the proton signals of β-CD and ester functions. This result is indicative of the fact that there is no appreciable hydrolysis of the ester bonds within the cross-linked polymer network, despite the fact that the pH of the mixture increases up to 8.1 during the NP synthesis (Fig. 1).

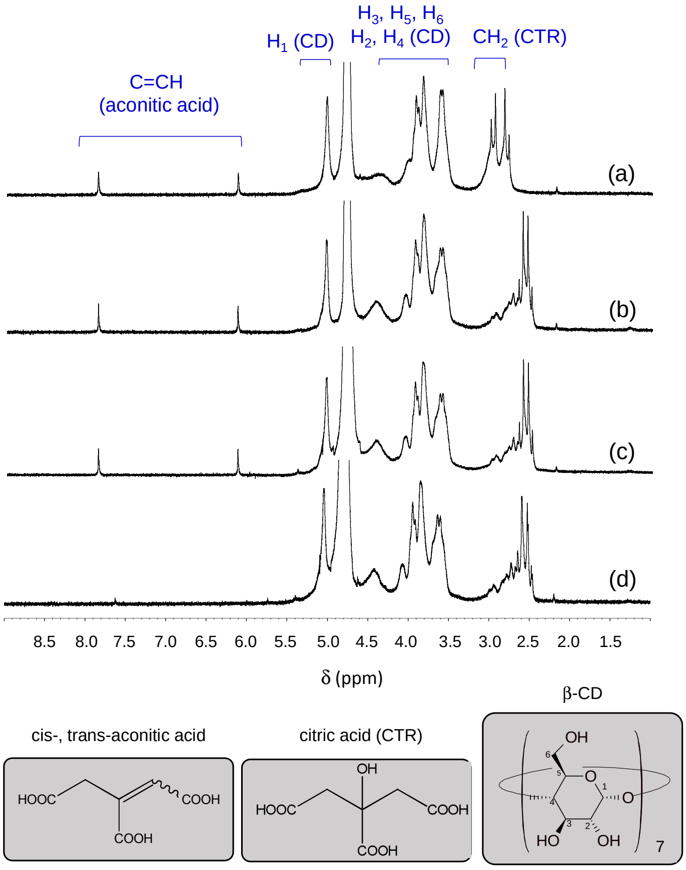

Fig. 1 ^1H NMR analysis in D_2O of poly(CTR-β-CD) after addition of the different reactants used for the synthesis of Ru(0) NPs: (a) Pristine poly(CTR-β-CD); (b) poly(CTR-β-CD) with $NaHCO_3$; (c) poly(CTR-β-CD) with $NaHCO_3$ and $Ru(NO)(NO_3)_3$ and (d) poly(CTR-β-CD)with $NaHCO_3$, $Ru(NO)(NO_3)_3$ and $NaBH_4$.

The absence of shift associated to the β-CD protons supports the view that the interactions between β-CD and ruthenium species are relatively weak, in agreement with a recent study reporting that the common cyclodextrins generally act as dispersing steric agents for the stabilization of NPs.[41,42] It can be further noted that the two singlets at $\delta = 6.11$ and 7.85 ppm characteristic of the olefinic proton of the *cis* and *trans* aconitic esters are absent from the spectrum measured with poly(CTR-β-CD) Ru(0) NPs (Fig. 1, spectrum d), and this can be related to the ability of zerovalent ruthenium to hydrogenate double bonds in unsaturated compounds. Comparison with a control spectrum of poly(CTR-β-CD) with $NaHCO_3$ and $NaBH_4$, but without addition of ruthenium salt, has clearly established that the reduction of the C=C double bonds occurred in the presence of metal (Fig. S2, spectrum e in the Supporting Information). It is also shown that the addition of $NaHCO_3$ to poly(CTR-β-CD) gives rise in all cases to a low-field shift of the proton NMR signals of the CH_2 groups belonging to the cross-linked chains caused by the deprotonation of the carboxylic acid groups to the negatively-charged carboxylate groups (Fig. 1, spectra b to d).

Evidence of the impact of the structure of poly(CTR-β-CD) to stabilize monodisperse ruthenium nanoparticles has been highlighted by TEM analysis at different magnifications (Fig. 2). The TEM image in Fig. 2a reveals that the Ru(0) nanoparticles assembled in water with poly(CTR-β-CD) are incorporated within superstructures forming discrete globules of more or less spherical shape. The size of the superstructures has been estimated to be mostly in the range of 50 to 100 nm in diameter. More specifically, these globular objects are composed of a large number of confined size-controlled metal nanoparticles, as illustrated in Fig. 2b. The corresponding particles surface density in the poly(CTR-β-CD) Ru(0) sample has been measured by counting ca. 600 particles from representative micrographs of spherical superstructures (Fig. S3 in the Supporting Information). The results indicate that the density is relatively uniform in each aggregate, approximately comprised of 50,000 to 80,000 nanoparticles per μm^2. A more detailed examination carried out at a higher magnification shows that small Ru nanocrystals isolated within the polymer matrix are obtained (Fig. 2c), with a narrow size distribution centered at 1.76 ± 0.32 nm (Fig. 2d). Indeed, we can see that ca. 90 % of the particles have a size between 1.5 and 2.5 nm and no particles larger than 3.25 nm can be found. Specifically, crystalline domains are shown in Fig. 2e with the presence of distinct lattice planes, which can be further analyzed by reduced fast Fourier transform (FFT)-derived diffraction patterns (Fig. 2f). The FFT-derived diffraction pattern indicates that the diffraction spot could be identified as ruthenium nanocrystals with a hexagonal close-packed structure, based on the reflection from the (101) planes having a typical d-spacing of 0.20 nm. The incorporation of ruthenium within the poly(CTR-β-CD) polymer has also been confirmed by electron microprobe analysis, with the appearance of its characteristic bands in the EDS spectrum. (Fig. S4 in the Supplementary material).

Note that the presence of aggregates of submicron size with narrow size distribution has been supported by additional dynamic light scattering measurements carried out on poly(CTR-β-CD) Ru(0) NPs. As evidenced in Fig. 3, the correlation function is a single exponential function indicating a monodisperse sample. The corresponding size distribution plot is monomodal with an apparent hydrodynamic diameter of the poly(CTR-β-CD) Ru(0) assemblies centred at ca. 80 nm.

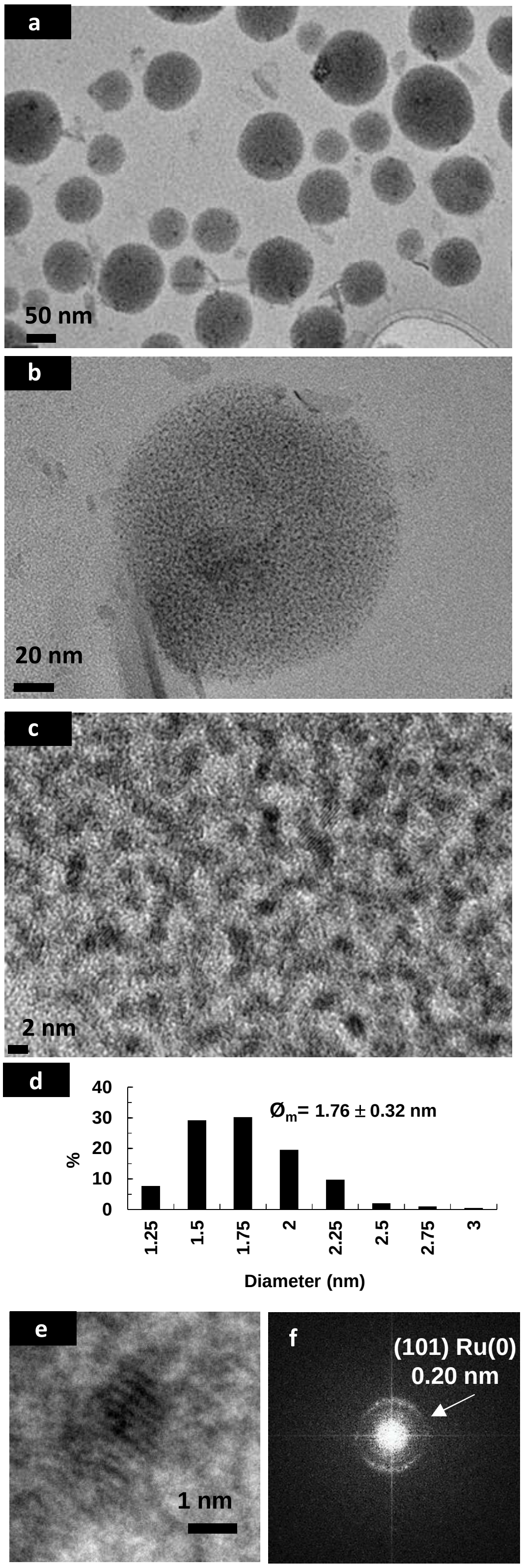

Fig. 2 TEM images of poly(CTR-β-CD) Ru(0) NPs at different magnifications: (a) 50 K. (b) 100 K. (c) 480 K. (d) Particle size distribution of the ruthenium NPs obtained from the measurement of ca. 200 particles. (e) TEM image of a single nanoparticle at a magnification of 700 K. (f) Reduced FFT-derived diffraction pattern in a typical crystalline region.

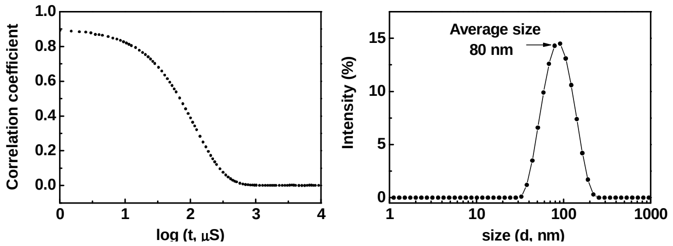

Fig. 3 Correlation function (left) and apparent hydrodynamic diameter distribution (right) of the scattered intensity for poly(CTR-β-CD) Ru(0) NPs colloidal suspension at 298 K.

In water, the ability of cross-linked cyclodextrin polymers to form under certain conditions porous nanoparticles of roughly spherical structures with a submicron size have already been observed by TEM measurements by Trotta and co-workers.[27] The mechanism, which limits the growth and regulates the shape is not well understood and possibly originates from surface-tension effect. However, it is expected that the presence of rigid cyclic β-CDs moieties covalently cross-linked to the polymer chains plays an important role for the specific distribution of the metal NPs within the cavities of the 3D-polymer structure. The formation of pockets result generally from the building up of the junction units, which are formed and stabilized through various interactions, such as hydrogen bonding or hydrophobic association. Thus when, during the synthesis of Ru(0) NPs, poly(CTR-β-CD) is substituted by another polymer, referred to as poly(CTR-MaltoD), prepared using the same polyesterification procedure as that previously described, except that maltodextrin (MaltoD; linear polysaccharide with a dextrose equivalent value of 19) is used instead of β-CD, ruthenium particles with a significant larger average particle size (3.79 ± 0.82 nm) and a broader size distribution (2-6 nm) are clearly produced (Fig. S5 in the Supporting Information). More importantly, it is worth emphasizing that no discrete spherical superstructures can be detected, but only branched wire-like assemblies, in which metal nanoparticles are attached to each other, are observed. Similar conclusions can be reached by using the sodium salt of CTR (molar ratio of COOH to $NaHCO_3$ = 1) as protective agent in the synthesis of Ru(0) NPs. Indeed, TEM pictures of the collected CTR-Ru(0) NPs show an average size of approximately 3.15 ± 0.60 nm (Fig. S6 in the Supporting Information). Additionally, the utilization of a simple mixture of CTR and β-CD in a non-polymerized state containing the same amounts of cyclodextrin moieties and COOH groups as those stated in the final poly(CTR-β-CD) polymer, results in a more densely packed morphologies of ruthenium particles with a higher polydispersity associated to the coexistence of small particles (2-3 nm) and large particles (> 20 nm) (Fig. S7 in the Supporting Information).

To evaluate the importance of the carboxylate groups on the stability of the poly(CTR-β-CD) Ru(0) colloidal suspension, we have performed other additional control experiments. First, it has been shown that the absence of pre-treatment of poly(CTR-β-CD) with $NaHCO_3$, prior to the reduction of the Ru^{3+} salt by $NaBH_4$, do not result in stable colloidal suspensions (the precipitation of black ruthenium is clearly observed at the end of the procedure). These results indicate that only large amounts of carboxylate groups present at the beginning of the synthesis can ensure appropriate conditions for the controlled nucleation of ruthenium nanoparticles, probably by establishing electrostatic interactions with the Ru^{3+} metal centers, themselves dispersed within the cross-linked β-CD polymer. The final pH is also an important factor that affects the stability of the aqueous suspensions containing ruthenium NPs (Fig. S8 in the Supporting Information). Indeed, its influence has been investigated by adjusting the pH in the range of 2-10 *via* the controlled addition of acid or base reagents (HCl or NaOH) to suspensions of poly(CTR-β-CD) Ru(0) NPs, whose synthesis has been described earlier. Therefore, we estimate that the stability of the colloids can be maintained by adjusting the pH to 5.0 or higher and this range is consistent with the almost complete dissociation of the carboxylic acid groups (≥ 90 %). Under such conditions and on the basis of the ruthenium content initially incorporated into the polymer, it can be concluded that the protective action of poly(CTR-β-CD) occur when the ratio COO^- to Ru is very high (above ca. 9). This is in good agreement with the literature,[43,44] where it has already been reported that sodium acetate could be used to control accurately the particle size of ruthenium NPs in polyol phases, provided that sodium acetate was added in sufficient amounts.

Taken together, these results indicate that the presence of carboxylate groups provide sites of interaction with the positively charged metal ion (Ru^{3+}), which are known to play an important role during the nucleation of metal clusters in the initial stages of reduction. In addition, it can be also assumed that the carboxylates exert a negative charge to the globule surfaces, establishing mutual electrostatic repulsion that contribute to their stabilization. This assumption has been further supported by zeta potential measurements of the aqueous suspensions of poly(CTR-β-CD) Ru(0) NPs. This technique is considered to be a useful indicator to evaluate the balance between the repulsive and attractive forces in solid suspensions. Poly(CTR-β-CD) Ru(0) NPs shows zeta potential values of -30.2, -33.4 and - 33.8 mV at pH = 5, 8 and 10, respectively. This range of negative values indicate that the colloidal suspensions can be classified as physically stable while the small shift in potential observed at pH 8-10 can be related to a slightly greater accumulation of carboxylate groups of the globules.

Catalytic hydrogenation

The catalytic activity of the colloidal suspension made of poly(CTR-β-CD) Ru(0) NPs and its different controls has been first evaluated in the aqueous hydrogenation of 2-furaldehyde Catalytic tests have been conducted in a stainless steel autoclave at 303 K under a dihydrogen pressure of 1 MPa and the reaction kinetic was monitored by gas chromatography (procedure in the experimental section). The results of the catalytic runs after 1.5 h reaction are summarized in Table 1.

Table 1 Influence of the nature of the protective agent of the Ru(0 NPs for the catalytic hydrogenation of 2-furaldehyde [a]

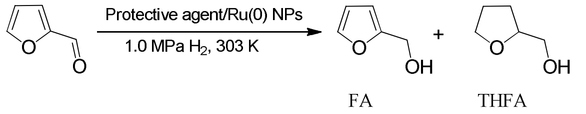

Entry	Stabilizer [b]	Conv. (%)	Selectivity (%)	
			FA[c]	THFA[c]
1	poly(CTR-β-CD)[c]	62	95	5
2	poly(CTR-MaltoD)[c]	16	100	0
3	CTR[e]	33	93	7
4	PM(CTR+β-CD)[c]	38	96	4
5	PVP-K30[e]	28	96	4
6	Ru/Al_2O_3[g]	13	95	5
7	Ru/C[g]	5	85	5

[a] *Reaction conditions*: Ru (40 µmol, 1 equiv.), 2-furaldehyde (2 mmol, 50 equiv.), H_2 (1.0 MPa), solvent (H_2O, 12 mL), stirring rate (1400 rpm), temperature (303 K), reaction time (1.5 h).[b] stabilizer previously treated with $NaHCO_{3(aq)}$ at a molar ratio of $NaHCO_3$ to COOH of 1 before the reduction of the ruthenium(III) salt (except for the Entry 5). [c] FA for furfuryl alcohol and THFA for tetrahydrofurfuryl alcohol. [d] 100 mg of cross-linked polymer or physical mixture of CTR and β-CD (50/50 wt./wt. %). [e] 50 mg of CTR. [f] 35.2 mg of PVP-K30 used as received (300 µmol, 7.5 equiv.). [g] 80 mg of commercial supported Ru catalyst used as received (5 wt. %).

When comparing the conversion of 2-furaldehyde over the different samples, it is readily apparent that the ruthenium nanoparticles stabilized within the cross-linked β-CD polymer is by far the most active system. It is worth mentioning here that the effect of β-CD within the poly(CTR-β-CD) Ru(0) system cannot be connected to the usual ability of β-CD to enhance mass transfer rates during catalytic processes.[45,46] Indeed, no inclusion complex between β-CD and 2-furaldehyde could have been observed by ^{1}H NMR. Thus, the poly(CTR-β-CD) Ru(0) NPs reach 62 % conversion after 1.5 h (Entry 1, Table 1) whereas, after the same period, the three control citrate-based ruthenium catalysts prepared from poly(CTR-MaltoD), CTR alone and PM(CTR+β-CD) (referred to as the physical mixture between CTR and β-CD without polymerization) show significant lower conversions, i.e. 16 % (Entry 2, Table 1), 33 % (Entry 3, Table 1) and 38 % (Entry 4, Table 1), respectively. However it should be noted that the latter system prepared by physical mixture cannot be considered as an efficient stabilizer of Ru(0) NPs since a black precipitate is observed at the end of the reaction, compromising therefore their reusability. The product distribution indicates in all cases the preferential formation of the unsaturated furfuryl alcohol (FA) with selectivity ranging from 93 to 100 %.For comparison, another colloidal system obtained by chemical reduction of $RuCl_3 \cdot 3H_2O$ with $NaBH_4$ in the presence of poly(N-vinyl-2-pyrrolydone) (PVP-K-30, MW= 58000) was also used as reference catalyst.[20,47,48] The corresponding average particle size is 2.95 ± 0.84 nm.[20] When these PVP Ru(0) nanoparticles were exposed to furfural hydrogenation, the reaction proceeds slowly, achieving a conversion level of 28 % (Entry 5, Table 1), which is 2.2 times lower than that of poly(CTR-β-CD) Ru(0) NPs. Concurrently to these ruthenium colloidal systems, commercial heterogeneous catalysts such as Ru/Al_2O_3 (5 wt. %) and Ru/C (5 wt. %) have also been evaluated as controls in this reaction, by keeping constant the metal content and therefore the substrate to metal ratio (Fig. S9 in the Supporting Information). Thus after 1.5 h reaction, hydrogenation of 2-furaldehyde yielded 13 % conversion (Entry 6, Table 1) and 5 % conversion (Entry 7, Table 1) for Ru/C and Ru/Al_2O_3 respectively, without affecting the selectivity (94-95% FA). The latter results are in agreement with the high-throughput screening of various alumina-supported monometallic catalysts performed by Huber and coworkers, who reported a moderate initial activity with their 3 % Ru/Al_2O_3 catalyst.[49] The use of Ru/C catalysts was also examined by different research groups in the hydrogenation of 2-furaldehyde in water.[50,51] Thus Ordomsky et al. showed that, while the initial reaction step mainly proceeds with the formation of FA, a number of hydrogenolysis by-products, such as 1,4-pentanedione, 1-hydroxy-4-pentanone or cyclopentanone, were formed through ring opening and/or rearrangement reactions.[51.] Finally, these comparisons are indicative of the difficulty of hydrogenating selectively 2-furaldehyde to FA and THFA with the use of conventional supported ruthenium catalysts, thus highlighting the result obtained with poly(CTR-β-CD) Ru(0) NPs. Note also that the level activity of poly(CTR-β-CD) Ru(0) NPs is of the same order of magnitude as that reported by Liaw et al. on NiB nanoparticle catalysts, but under more severe conditions (T = 353 K, P(H_2) = 1.8 MPa).[52,53]

Taken together, our results show that the hydrogenation activity of the aforementioned colloidal catalysts can be generally correlated with the average size of the ruthenium particles. Indeed, the best results are obtained with the use of poly(CTR-β-CD) allowing the stabilization of the smallest Ru(0) clusters of the series, i.e. 1.76 nm. In addition, the arrangement of these metal NPs in the surrounding protective microenvironment has also to be considered as an important factor that affects their ability to expose a large fraction of active sites. The utilization of the polymer formed by the crosslinking of β-CD with CTR provides isolated micrometer-scale globular assemblies that promote the confinement and dispersion of high density size-controlled Ru(0) NPs but also the product/substrate diffusional exchanges between the globule and bulk solution. Thus, the rigidity and steric hindrance of β-CD caused by the cyclic arrangement of the seven glucose units is suggested to play a critical role for ensuring good diffusion of the reactant. This idea is further supported by the fact that a much lower activity is observed for the Ru(0) NPs stabilized by poly(CTR-MaltoD) compared to those by poly(CTR-β-CD). This result may be correlated to a greater flexibility of the linear structure of maltodextrin, presumably responsible for the formation of less well-defined cavities in the 3D-polymer network (related to the numerous hydroxyl groups that can be randomly and differently involved during the polyesterification process).

To validate the stabilization with poly(CTR-β-CD), we have extended the time of reaction to complete the hydrogenation reaction. Fig. 4 shows the reaction profile for the hydrogenation of 2-furaldehyde over poly(CTR-β-CD) Ru(0) NPs at 303 K.

The profile illustrates the sequential nature of the reaction as furfural is first hydrogenated to the unsaturated furfuryl alcohol (constant selectivity of ca. 95 %), which is subsequently hydrogenated to form the saturated tetrahydrofurfuryl alcohol. Interestingly, the saturated alcohol is produced only after all furfural is converted to the intermediate furfuryl alcohol, i.e. after 3 h reaction. Notably, the rate of reduction of the endocyclic double bonds is found to be much faster than that of the aldehyde. Thus, 2-furaldehyde is completely hydrogenated to the saturated alcohol with 100 mol % yield in 4 h with poly(CTR-β-CD) Ru(0) NPs without any loss of stability, whereas much time is necessary with the other Ru-based systems. A standard isolation procedure of successive extractions with chloroform (total volume doubling the water extract) provides an isolated yield of 83 %. As comparative examples, it can be noticed that the yield of THFA does not exceed 3 mol % and 10 mol % after 4 h reaction time, when the reaction is carried out in the presence of CTR and PM(CTR+β-CD Ru(0) NPs, respectively (Fig. S10 and Fig. S11 in the Supporting Information).

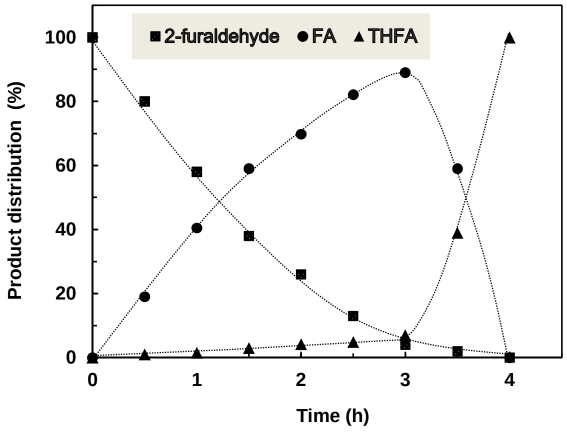

Fig. 4 Reaction profile for the hydrogenation of 2-furaldehyde over polyCTR-β-CD Ru(0) NPs: 2-furaldehyde (■), furfuryl alcohol (●) and tetrahydrofurfuryl alcohol (▲). *Reaction conditions*: Ru (40 µmol, 1 equiv.), 2-furaldehyde (2 mmol, 50 equiv), H_2 (1.0 MPa), solvent (H_2O, 12 mL), stirring rate (1400 rpm), temperature (303 K), reaction time (4 h).

In order to extend the scope of poly(CTR-β-CD) Ru(0) as catalyst, the hydrogenation of 3-(2-furyl)acrolein has also been examined. This furan derivative can be produced by an aldol condensation of furfural with acetaldehyde and, in addition can be considered as a heterocyclic analogue of cinnamaldehyde. Recently, the aldol approach has given access to a range of furaldehyde-based derivatives and has opened a general integrated strategy for the synthesis of medium-chain-length alcohols from carbohydrate feedstock (through hydrogenation and selective deoxygenation /ring opening processes).[54,55] However, the aldol condensation products, such as 3-(2-furyl)acrolein are solid at ambient temperatures and their solubility in water is extremely low, preventing adequate mass-transfer. To overcome this limitation, 3-(2-furyl)acrolein has to be solubilized in absolute ethanol[56,57] (12 mL) before carrying out the hydrogenation tests in the same conditions of temperature and pressure as those previously described (303 K, 10 MPa H_2). Scheme 3 shows the possible products resulting from the hydrogenation of 3-(2-furyl)acrolein. The first hydrogenation products are either the aldehyde (1) or unsaturated alcohol (2) formed by the hydrogenation of the C=C bond or C=O bond, respectively. These compounds can be further hydrogenated to successively produce the intermediate (2-furyl)propan-1-ol (3) and the fully saturated alcohol (4).

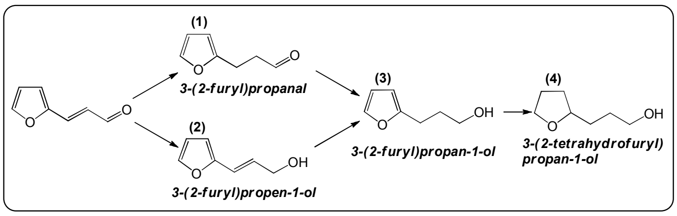

Scheme 3 Proposed reaction pathway for the hydrogenation of 3-(2-furyl)acrolein

Table 2 reports the catalytic performances of the poly(CTR-β-CD) Ru(0) NPs after 1.5 h reaction and, for comparison, results achieved in the presence of ruthenium controls are also given. Notably, the results show a similar tendency as that observed for the hydrogenation of furfural. Indeed, it is clearly evidenced that the use of poly(CTR-β-CD) in the stabilization of Ru(0) NPs affects positively the reactivity since the level of conversion of 38 % is 2 to 4.75 times higher than that measured with the other ruthenium systems (Entry 1, Table 2). Whatever the Ru(0) NPs system, the unsaturated aldehyde (1) is the main product at this reaction time (selectivity = 87-96 %) and no trace of the unsaturated alcohol intermediate (2) has ever been found. This result is not surprising given that the addition of hydrogen to a conjugated C=C bond is thermodynamically favoured over the C=O bond.[58]

Table 2 Influence of the protective agent on the catalytic hydrogenation of 3-(2-furyl)acrolein with Ru(0) NPs [a]

Entry	Stabilizer[b]	Conv. (%)	Selectivity (%)			
			(1)	(2)	(3)	(4)
1	poly(CTR-β-CD)[c]	38	87	0	13	0
2	poly(CTR-MaltoD)[c]	15	90	0	10	0
3	CTR[d]	18	96	0	4	0
4	PM(CTR+β-CD)[c]	19	93	0	7	0
5	PVP-K30[e]	8	93	0	7	0

[a] *Reaction conditions*: Ru (40 µmol, 1 equiv.), 3-(2-furyl)acrolein (2 mmol, 50 equiv), H_2 (1.0 MPa), H_2O, (12 mL), ethanol (12 mL), stirring rate (1400 rpm), temperature (303 K), reaction time (1.5 h).[b] stabilizer previously treated with $NaHCO_{3(aq)}$ at a molar ratio of $NaHCO_3$ to COOH of 1 before the reduction of the ruthenium(III) salt (except for the Entry 5).[c] 100 mg of cross-linked polymer or physical mixture of CTR and β-CD (50/50 wt./wt. %). [d] 50 mg of CTR. [e] 35.2 mg of PVP-K30 used as received (300 µmol, 7.5 equiv.)

Considering the best behaviour of the poly(CTR-β-CD) Ru(0) NPs and in order to provide a better insight into the reaction mechanism, a kinetic experiment has been finally conducted (Fig. 5). The kinetic curve reveals that the hydrogenation of 3-(2-furyl)acrolein in the presence of colloidal nanoparticles occurs in three consecutive steps, as mentioned above. Thus, it is observed that 3-(2-furyl)acrolein is first converted to 3-(2-furyl)propanal (1), which is subsequently hydrogenated to 3-(2-furyl)propan-1-ol (3). The last step (very fast) is the hydrogenation of the heteroaromatic ring leading to the fully saturated alcohol product (4). Interestingly, the consecutive reaction mechanism over the poly(CTR-β-CD) Ru(0) system allows accessing the unsaturated alcohol (3) or saturated alcohol (4) in high selectivities *via* the hydrogenation of 3-(2-furyl)acrolein. The reaction is completed (100 mol % yield) after 7.5 h reaction, without any signs of destabilization of the poly(CTR-β-CD) Ru(0) colloidal suspension.

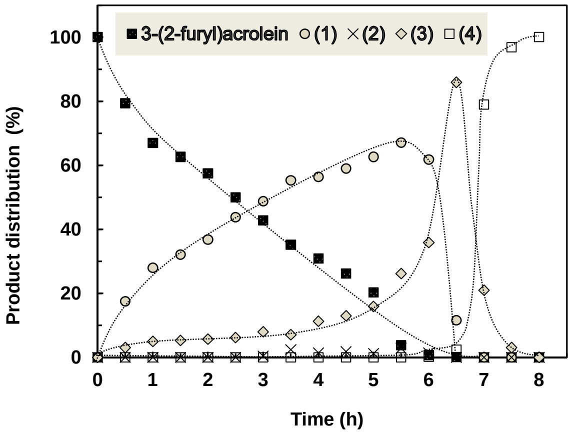

Fig. 5 Reaction profile for the hydrogenation of 3-(2-furyl)acrolein over polyCTR-β-CD Ru(0) NPs: 3-(2-furyl)acrolein (■), 3-(2-furyl)propanal (1), 3-(2-furyl)propen-1-ol (2), 3-(2-furyl)propan-1-ol (3) and 3-(2-tetrahydrofuryl)propan-1-ol (4). *Reaction conditions*: Ru (40 µmol, 1 equiv.), furfural (2 mmol, 50 equiv.), H_2 (1.0 MPa), H_2O, (12 mL), ethanol (12 mL), stirring rate (1400 rpm), temperature (303 K), reaction time (8 h).

Recycling

The reusability of poly(CTR-β-CD) Ru(0) NPs has been specifically investigated on 2-furaldehyde at 1 MPa H_2 and 303 K. After a first run with the fresh catalytic system (4 h) and complete conversion of 2-furaldehyde (> 95 %), the catalyst is thoroughly washed with diethyl ether until complete elimination of the reaction product. After removal of the remaining diethyl ether under vacuum, the aqueous colloidal suspension is reloaded with 2-furaldehyde and dihydrogen and reused in hydrogenation as in the initial run. Fig. 6 clearly exhibits that the colloidal suspension made of poly(CTR-β-CD) Ru(0) NPs is stable and reusable under the reaction conditions, preserving its activity on the hydrogenation of 2-furaldehyde to tetrahydrofurfuryl alcohol after 5 consecutive runs. Moreover, it is worth mentioning that the stability of the poly(CTR-β-CD) Ru(0) system has been checked by TEM measurements. Thus, the picture taken after reaction clearly shows that the discrete superstructures encapsulating the metal nanoparticles are maintained without any apparent change of morphologies. Notably, the Ru(0) NPs displays a Gaussian-like distribution and a mean diameter of 1.87 nm with 95 % between 1.5 and 2.5 nm is obtained, correlating with the data obtained before catalysis (Fig. S12 in the Supporting Information). This last result gives a strong indication of the resistance of the ruthenium nanoparticles under the catalytic conditions used for the hydrogenation of furan derivatives compounds, when they are dispersed within the protective large superstructures formed by poly(CTR-β-CD). Further evidence of the fact that the chemical structure of the polymer network is not altered during catalysis and product extraction has been also obtained by ^1H NMR measurements (Fig. S13 in the Supporting Information). Finally, the enhanced catalytic stability and performances can be attributed to the ability of this cross-linked polymer to provide a good balance of stabilizing properties with the metal surface, both in terms of steric interactions (polymer and β-CD) and electrostatic interactions (ionisable–COOH groups), without hindering the catalytic activity.

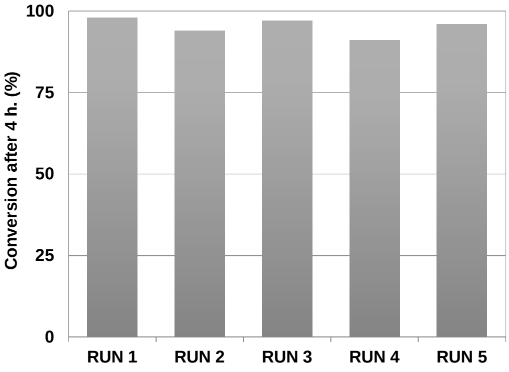

Fig. 6. Reusability of poly(CTR-β-CD) Ru(0) NPs in the hydrogenation of 2-furaldehyde. *Reaction conditions*: Ru (40 µmol, 1 equiv.), 2-furaldehyde (2 mmol, 50 equiv.), H_2 (1.0 MPa), solvent (H_2O, 12 mL), stirring rate (1400 rpm), temperature (303 K), reaction time (4 h).

Conclusions

In conclusion, we have described the synthesis and characterization of water-dispersible ruthenium nanoparticles utilizing a three-dimensional β-cyclodextrin polymer (prepared by polycondensation between native β-CD and citric acid) as a novel stabilizer. Ruthenium was introduced by using ruthenium nitrosyl nitrate while the stability of the ruthenium colloids was profoundly affected by the acid or alkaline nature of the polymer aqueous solution. Under appropriate conditions of pH, TEM revealed that the use of poly(CTR-β-CD) led to the formation of generally spherical, discrete superstructures of ca. 50-100 nm in diameter, which are composed of a large number of individual ruthenium nanoparticles with a narrow size-distribution centered around 1.8 nm. These embedded ruthenium nanoparticles were successfully applied as efficient and reusable catalysts for the aqueous phase hydrogenation of furan-derived compounds, such 2-furaldehyde and 3-(2-furyl)acrolein. This easy approach contributes to provide a generation of more robust colloidal catalysts, allowing not only the confinement of catalytically active nanoparticles but also the diffusional exchanges between the microcapsule and the bulk solution. These features are known to be key factors in heterogeneous catalytic processes.

Experimental

General

$Ru(NO)(NO_3)_3$ solution (1.5 wt. % Ru) was purchased from STREM chemicals. 2-furaldehyde was purchased from Aldrich Chemicals and was used after distillation under vacuum. 3-(2-furyl)acrolein, sodium borohydride, citric acid and sodium hydrogenocarbonate were obtained from Acros Organics and Aldrich Chemicals and were used without any further purification. Absolute ethanol was purchased from Fisher Scientific. β-CD and Glucidex®Maltodextrin 19 (dextrose equivalent 19) were generous gifts from Roquette Frères (Lestrem, France). Poly(CTR-β-CD) and poly(CTR-MaltoD) polymers have been synthesized by polyesterification in the presence of citric acid according to a previously reported procedure.[35] Two commercially available supported ruthenium catalysts, Ru/C (5 wt. %) and Ru/Al_2O_3 (5 wt. %), were supplied by Aldrich Chemicals and used as received. Purified deionised water from Fresenius Kabi was used as aqueous solvent.

Synthesis of colloidal Ru(0) nanoparticles

In a typical experiment, the colloidal suspension was prepared as follows at ambient temperature. 100 mg of poly(CTR-β-CD) (MW = 25000, 4.05 mmol g^{-1} COOH acidic sites) were dissolved in 5 mL of deionized water in the presence of a controlled amount of $NaHCO_3$ (molar ratio of $NaHCO_3$ to COOH = 1) and the mixture is kept under vigorous stirring during 3 h. Then 269 mg of $Ru(NO)(NO_3)_3$ solution (1.5 wt.% Ru) (40 μmol, 1 equiv.) were dispersed in 3 mL of deionized water. The both solutions were mixed together under vigorous stirring during 30 minutes. Then, 15.2 mg of $NaBH_4$ (400 μmol, 10 equiv.) previously dissolved in 4 mL of water were quickly added to the mixture. The resulting colloidal suspension was kept under vigorous stirring for 24 hours in order to check that there is no sedimentation of the metallic particles before the beginning of the catalytic test.

NMR analysis

The ^1H spectra were recorded at 300.13 MHz on a Bruker Avance DRX300 spectrometer. D_2O (99.92%, isotopic purity) was purchased from Euriso-Top. The ^1H chemical shifts are given in parts per million (ppm) relative to the trimethylsilyl-3-propionic acid-d_4-2,2,3,3 sodium salt (98% atom D) in D_2O using internal capillary.

TEM analysis

Transmission Electron Microscopy (TEM) was performed on a Tecnai microscope (200 kV). A drop of the colloidal suspension was deposited on a carbon coated copper grid. The size distribution of the nanoparticles was estimated after the measurement of 200 particles with the program SCION Image. Particle density distribution was determined with the program SCION Image by using ca. 600 Ru(0) NPs selected in multiple regions of the TEM images with surface areas ranging from 300 to 400 nm^2.

Zeta Potential analysis

Zeta potential measurements were carried out in water suspension using a Malvern Zetasizer Nano ZS. The ξ-potential corresponds to the potential difference between the dispersion medium and the electrical double layer of fluid attached to the dispersed particle. The measurements are based on a Laser Doppler electrophoretic mobility of metallic nanoparticles *via* the Helmholtz–Smoluchowski equation, $\xi=(\eta/\varepsilon)\bullet\mu_e$, where μ_e is defined as the ratio between the velocity of the metallic nanoparticles and the magnitude under the applied electric field, η is the viscosity of the suspending liquid and ε the dielectric conductivity of water. The colloidal suspensions were analyzed without any previous treatment.

General procedure for the hydrogenation of 2-furaldehyde

The stainless steel autoclave was charged with 12 mL of the standard colloidal suspension of Ru(0) (40 μmol, 1 equiv.). Then 50 equiv. of 2-furaldehyde was added into the autoclave and hydrogen was admitted to the system at constant pressure up to 1.0 MPa. The mixture was heated to 303 K and stirred at 1400 rpm. At regular time intervals, precise volumes of sample were withdrawn from the reaction mixture (500 μL) and subjected to direct organic extraction with diethy ether (2 mL). The reaction was then monitored by analyzing these aliquots using a Shimadzu GC-17A gas chromatograph, equipped with a methyl silicone capillary column (30 m × 0.32 mm) and a flame ionization detector. Conversions, selectivities and GC yields were quantified by gas chromatography, based on the relative GC-areas referred to an external standard (decane) calibrated to the corresponding pure compounds.

For the recycling procedure, after complete conversion of furfural, the hydrogenation products were extracted by liquid-liquid extraction and decantation with diethyl ether. Then after elimination of the organic phase under vacuum, the colloidal suspension was reloaded with 2-furaldehyde and dihydrogen and reused in hydrogenation in the autoclave as described above.

General procedure for hydrogenation of 3-(2-furyl)acrolein

The catalytic tests for the hydrogenation of 3-(2-furyl)acrolein have been carried out in a similar manner as that previously described for the hydrogenation of 2-furaldehyde, except that the 50 equiv. of 3-(2-furyl)acrolein were solubilized into 12 mL of absolute ethanol.

Acknowledgments

The TEM facility in Lille (France) is supported by the Conseil Regional du Nord-Pas de Calais and the European Regional Development Fund (ERDF). We thank Grégory Crowyn and Dr. Antonio Da Costa from the University of Artois for their help with NMR and TEM measurements, respectively. R.H. is grateful to the Ministère de l'Education Nationale, de l'Enseignement Supérieur et de la Recherche for the Ph.D. grant.

Notes and references

[a] Université d'Artois, Unité de Catalyse et de Chimie du Solide (UCCS), Faculté des Sciences Jean Perrin, Rue Jean Souvraz, SP 18, F-62307 Lens Cedex, France.
[b] CNRS, UMR 8181, F-59650 Villeneuve d'Ascq, France
[c] Université de Lille, UMET, UMR 8207, F-59650 Villeneuve d'Ascq, France

† Preliminary experiments showed that the most suitable molar ratio of $NaBH_4$ to ruthenium required to form stable Ru(0) nanoparticle was 10 in the presence 100 mg of poly(CTR-β-CD) (normal experimental conditions). Incomplete reduction of Ru(III) ions was observed using a ratio of Ru to $NaBH_4$ smaller than 10 whereas a ratio higher than 12.5 led to the agglomeration of the Ru(0) nanoparticles (under catalytic reaction conditions, i.e. 1 MPa H_2).

Electronic Supplementary Information (ESI) available: [Acid-base titration curve of poly(CTR-β-CD) (Fig. S1). ^{1}H NMR analysis in D_2O of poly(CTR-β-CD) after addition of different reactants (Fig. S2). TEM characterization for the surface density calculation of Ru(0) NPs in poly(CTR-β-CD) (Fig. S3). EDS spectrum of poly(CTR-β-CD) Ru(0) NPs (Fig. S4). TEM analysis of the series of control colloidal catalysts (Figs S5-S7). Percent of carboxylic acid groups and carboxylate to ruthenium ratios in the poly(CTR-β-CD) *vs* pH (Fig. S8). Conversion of 2-furaldehyde as a function of time over Ru/C and Ru/Al_2O_3 control catalysts: (Fig. S9). Reaction profiles for the 2-furaldehyde hydrogenation over CTR-β-CD Ru(0) NPs (Fig. S10) and PM(CTR+β-CD) Ru(0) NPs (Fig. S11). TEM characterization of poly(CTR-β-CD) Ru(0) NPs after test (Fig. S12). ^{1}H NMR spectrum of poly(CTR-β-CD) Ru(0) NPs dispersed in D_2O (before and after catalysis) (Fig. S13)]. See DOI: 10.1039/b000000x/

1 A. Roucoux, J. Schulz and H. Patin, *Chem. Rev.*, 2002, **102**, 3757.
2 Nanoparticles and Catalysis, ed. D. Astruc, Wiley-VCH, Weinheim, 2007.
3 N. Yan, C. Xiao and Y. Kou, *Coord. Chem. Rev*., 2010, **254**, 1179.
4 M. Zahmakırana and S. Özkar, *Nanoscale*, 2011, **3**, 3462.
5 J.W Yoo, D.J. Hathcock and M.A. El-Sayed, *J. Catal*., 2003, **214**, 1.
6 A. Denicourt-Nowicki, A. Roucoux, F. Wyrwalski, N. Kania, E. Monflier and A.Ponchel, *Chem. Eur. J*., 2008, **14**, 8090.
7 F. Wyrwalski, B. Léger, C. Lancelot, A. Roucoux, E. Monflier and A.Ponchel, *Appl. Catal. A.: Gen*., 2011, **391**, 334.
8 L.M. Bronstein, G. Goerigk, M. Kostylev, M. Pink, I.A. Khotina, P. M. Valetsky, V.G. Matveeva, E.M. Sulman, M.G. Sulman, A.V. Bykov, N.V. Lakina and R.J. Spontak, *J. Phys. Chem. B*, 2004, **108**, 18234.
9 A. Nowicki, V. Le Boulaire and A. Roucoux, *Adv. Synth. Catal*. 2007, **349**, 2326.
10 D. Gonzalez-Galvez, P. Nolis, K. Philippot, B. Chaudret and P.W.N.M. van Leeuwen, *ACS Catal*., 2012, **2**, 317.
11 C.Zhao, W. Gan, X. Fan, Z. Cai, P.J. J. Dyson and Y. Kou, *J. Catal*., 2008, **254**, 244.
12 A.B.R. Mayer and J.E. Mark, *Coll. Polym. Sci*., 1997, **275**, 3.
13 M.V. Seregina, L.M. Bronstein, O.A. Platonova, D.M. Chernyshov, P.M. Valetsky, J. Hartmann, E. Wenz and M. Antonietti, *Chem. Mater*., 1997, **9**, 923.
14 P. Alexandridis and M. Tsianou, *Eur. Polymer J*., 2011, **47**, 569.
15 Y. Li and M.A. El-Sayed, *J. Phys. Chem. B*, 2001, **105**, 8938.
16 N.C. Antonels and R. Meijboom, *Langmuir*, 2013, **29**, 13433
17 D. Astruc, E. Boisselier and C. Ornelas, *Chem. Rev*., 2010, **110**, 1857.
18 L.D. Pachón and G. Rothenberg, *Appl. Organometal. Chem*., 2008, **22**, 288.
19 M.A.R. Meier, M. Filali, J. F. Gohy and U.S. Schubert, *J. Mater. Chem*., 2006, **16**, 3001.
20 R. Herbois, S. Noël, B. Léger, L. Bai, A. Roucoux, E. Monflier and A. Ponchel, *Chem. Commun*., 2012, **48**, 3451.
21 S. Noël, B. Léger, R. Herbois, A. Ponchel, S. Tilloy, G. Wenz and E. Monflier, *Dalton Trans*. 2012, **41**, 13359.
22 S. Noël, B. Léger, A. Ponchel, K. Philippot, A. Denicourt-Nowicki, A. Roucoux and E. Monflier, *Catal Today*, 2014, **235**, 20.
23 S. Noël, B. Léger, A. Ponchel, F. Hapiot and E. Monflier, *Chem. Eng. Trans*., 2014, **37**, 337.
24 V. Wintgens and C. Amiel, *Eur. Polym. J.*, 2010, **46**, 1915.
25 M.J. Kutyla, L.K. Lambert, N.M. Davies, R.P. McGeary, P.N. Shaw and B.P. Ross, *Int. J. Pharm.*, 2013, **444**, 175.
26 D. Li and M. Ma, *Chem. Mater*., 1999, **11**, 872.
27 F. Trotta, M. Zanetti and R. Cavalli, *Beilstein J. Org. Chem*, 2012, **8**, 2091.
28 W. Liang, C. Yang, M. Nishijima, G. Fukuhara,T. Mori, A. Mele, F. Castiglione, F. Caldera, F. Trotta and Y. Inoue, *Beilstein J. Org. Chem*, 2012, **8**, 1305.
29 Y. Shiraishi, M. Hashimura, M. Nakao, T. Ishizu, M. Kazita, Y. Miyamoto and N. Toshima, *Supramol. Chem.*, 2011, **23**, 195.
30 M.J. Climent, A. Corma and S. Iborra, *Green Chem*., 2011, **13**, 520.
31 R. Alamillo, M. Tucker, M. Chia, Y. Pagán-Torres and J. Dumesic, *Green Chem*., 2012, 14, 1413
32 Y. Nakagawa, M. Tamura and K. Tomishige, *ACS Catal*., 2013, **3**, 2655.
33 M. Besson, P. Gallezot and C. Pinel, *Chem. Rev*., 2014, **114**, 1827.
34 S. Boufi, M.N. Belgacem, J. Quillerou, and A. Gandini, *Macromolecules*, 1993, **26**, 6706.
35 S. Boufi, A. Gandini and M.N. Belgacem, *Polymer*, 1995, **36**, 1689.
36 A. Gandini, and C. Méalares, *Trends Polym. Sci*., 1994, **2**, 127.
37 B. Martel, D. Ruffin, M. Weltrowski, Y. Lekchiri and M. Morcellet, *J. Appl. Polym. Sci.*, 2005, **97**, 433.
38 A. Martin, N. Tabary, L. Leclercq, J. Junthip, S. Degoutin, F. Aubert-Viard, F. Cazaux, J. Lyskawa, L. Janus, M. Bria and B. Martel, *Carbohyd. Polym.*, 2013, **93**, 718.
39 A. Nowicki, Y. Zhang, B. Léger, J.P. Rolland, H. Bricout, E. Monflier and A. Roucoux, *Chem. Commun*., 2006, **42**, 296.
40 A. Denicourt-Nowicki, A. Ponchel, E. Monflier and A. Roucoux, *Dalton Trans*., 2007, **36**, 5714.
41 N.T.T. Chau, S. Handjani, J-P. Guegan, M. Guerrero, E. Monflier, K. Philippot, A. Denicourt-Nowicki and A. Roucoux, *ChemCatChem*, 2013, **5**, 1497.
42 N.T.T. Chau, J-P. Guégan, S. Menuel, M. Guerrero, F. Hapiot, E. Monflier, K. Philippot, A. Denicourt-Nowicki and A. Roucoux, *Appl. Catal. A.: Gen*., 2013, **467**, 497.

43 G. Viau, R. Brayner, L. Poul, N. Chakroune, E. Lacaze,, F. Fiévet-Vincent and F. Fiévet, *Chem. Mater*., **2003**, 15, 486.

44 J. Yang, T.C. Deivaraj, H.P. Too and J.Y. Lee, *Langmuir*, 2004, **20**, 4241

45 F. Hapiot, A. Ponchel, S. Tilloy and E. Monflier, *C. R. Chimie*, 2011, 14, 149

46 F. Hapiot, H. Bricout, S. Menuel, S. Tilloy and E. Monflier, *Catal. Sci. Technol.*, 2014, **4**, 1899.

47 F. Lu, J. Liu and J. Xu, *Adv. Synth. Catal*., 2006, **348**, 857.

48 F. Lu, J. Liu and J. Xu, *J. Mol. Catal. A: Chem*., 2007, **108**, 6.

98.

49 J. Lee, Y. Xu and G.W. Huber, *Appl. Catal. B.: Environ*., 2013, **140-141**, 98

50 N. Merat, C. Godawa and A. Gaset, *J. Chem. Tech. Biotechnol.*, 1990, **48**, 145.

51 V.V. Ordomsky, J.C. Schouten, J. van der Schaaf and T.A. Nijhuis, *Appl. Catal*. A *: Gen*., 2013, **451**, 6.

52 B.J. Liaw, S.J. Chiang, C.H. Tsai and Y.Z. Chen, *Appl. Catal*. A *: Gen*., 2005, **284**, 239.

53 S.J. Sheng, B.J. Liaw and Y.Z. Chen, *Appl. Catal*. A *: Gen*., 2007, **319**, 144

54 J. Julis, M. Hölscher and W. Leitner, *Green Chem*., 2010, **12**, 1634.

55 J. Julis and W. Leitner, *Angew. Chem. Int. Ed*., 2012, **51**, 1.

56 R. Hoogenboom, H.M.L. Thijs, D. Wouters, S. Hoeppener and U.S. Schubert, *Soft Matter*, 2008, **4**, 103.

57 M.H. Abraham and W.E. Acree, *J. Solution Chem*., 2011, **7**, 1279.

58 G.C. Bond, Catalysis of Metals; Academic Press: London, 1962.

Ruthenium-containing β-cyclodextrin polymer globules for the catalytic hydrogenation of biomass-derived furanic compounds

R. Herbois,[a,b] S. Noël, [a,b] B. Léger,[a,b] S. Tilloy,[a,b] S. Menuel, [a,b] A. Addad,[c] B. Martel,[c] A. Ponchel,[a,b] and E. Monflier*[a,b]

[a] Université d'Artois, Unité de Catalyse et de Chimie du Solide (UCCS), Faculté des Sciences Jean Perrin, Rue Jean Souvraz, SP 18, F-62307 Lens Cedex, France.

[b] CNRS, UMR 8181, F-59650 Villeneuve d'Ascq, France

[c] Université de Lille, UMET, UMR 8207, F-59650 Villeneuve d'Ascq, France

Graphical Abstract

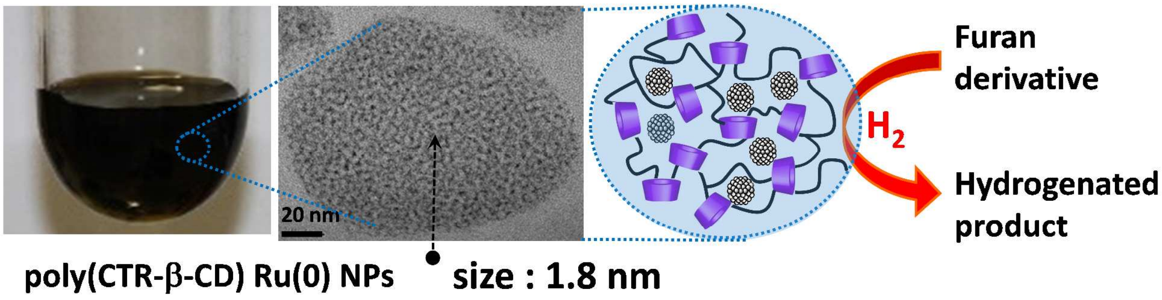

Robust and highly efficient ruthenium nanoparticles confined within individual microenvironments formed by a three-dimensional β-cyclodextrin polymer were easily prepared for the hydrogenation of biomass-derived furan compounds in water.